Heliyon 10 (2024) e36875

Contents lists available at ScienceDirect

Heliyon

journal homepage: www.cell.com/heliyon

Research article

Self-ignition behaviour of corn cob, wheat bran and rice husk residues in ambient air from biomass gasification

Moses Oshiomah Osibuamhe [a,**], Lekan Taofeek Popoola [b,c,*], Yuli Panca Asmara [c], Usman Taura [d], Tajudeen Adejare Aderibigbe [e]

[a] Faculty of Process and Systems Engineering, Institute of Apparatus and Environmental Technology, Otto-Von-Guericke University, Magdeburg, Germany
[b] Chemical and Petroleum Engineering Department, Afe Babalola University, Ado-Ekiti, Ekiti State, Nigeria
[c] INTI International University, FEQS, Nilai, 71800, Negeri Sembilan, Malaysia
[d] Oil and Gas Research Centre, Sultan Qaboos University, Oman
[e] Science Laboratory Technology Department, Yaba College of Technology, Yaba, Lagos State, Nigeria

ARTICLE INFO

Keywords:
Self-ignition temperature
Hazardous waste
Corn cob residue
Wheat bran residue
Rice husk residue

ABSTRACT

The possibility of different agrowastes to self-ignite under ambient condition, due to exothermic reactions between their surface molecules and air or other oxidizing agents which are conveyed into the void volume between the particles, exists. It is imperative to investigate the self-ignition ability of these harzadous waste products causing environmental pollution after the milling process to avoid sudden fire outbreaks. In this study, the self-ignition attributes of corn cob, wheat bran and rice husk residues in ambient air from biomass gasification was investigated by evaluating their self-ignition temperatures using DIN EN 15188:2021 standard and Frank-Kamenetzkii's theory of thermal explosion at varying basket volume. The results revealed decrease in the ignition temperature of dust samples as ignition time and dust basket volume were increased. Sample C (rice husk dust residue) was considered to be the most hazardous with respect to its propensity to self-heating possessing the lowest self-ignition temperature of 173 °C at 800 mL cubic mesh. Its moisture content and activation energy of 1.41 % and 46.52 kJ/mol respectively were the lowest. Its thermal conductivity, carbon content, heating value and bulk density of 0.07 W/mK, 78.98 wt%, 26,895 kJ/kg and 255.4 kg/m^3 respectively were the highest. Correlation coefficient from the Arrhenius plot showing the self-ignition behaviour of dust samples using the model of Frank-Kamenetzkii were 0.9976, 0.9910 and 0.9962 for corn cob, wheat bran and rice husk residues respectively. In conclusion, the data presented are effective in predicting the self-ignition ability of corn cob, wheat bran and rice husk residues in ambient air from biomass gasification in order to prevent sudden fire attack that may arise based on storage of their dust particles in food processing industries.

1. Introduction

Biomass are usually products, residues and wastes from biological agricultural origin which are biodegradable in nature [1,2]. They

* Corresponding authors. Chemical and Petroleum Engineering Department, Afe Babalola University, Ado-Ekiti, Ekiti State, Nigeria.
** Corresponding author.
E-mail addresses: moses.osibuamhe@st.ovgu.de (M.O. Osibuamhe), ltpopoola@abuad.edu.ng (L.T. Popoola).

https://doi.org/10.1016/j.heliyon.2024.e36875
Received 8 March 2024; Received in revised form 20 August 2024; Accepted 23 August 2024
Available online 25 August 2024

also include forestry and related industries including fisheries and aquaculture; vegetable and animal substances [3,4]; as well as the biodegradable fraction of industrial and municipal waste [5]. Accumulation of dust occurs on several occasions in different coal mills, wood mills and power plants [6] that handle, process or store dust and other bulk materials. In the presence of an oxidant, self-ignition of the accumulated dust may occur via the initiation of smoldering [7]. This can additionally generate hot spots which activate dust explosion [8]. Factors that determine the self-ignition of a combustible dust are the properties of the substance, ambient temperature, its chemical composition, size and geometry [9]. Historically, records of damages from fires via self-ignition of dust materials have been recorded [10]. As a result of these, numerous tests have been conducted on different materials that can spontaneously ignite to understand their tendencies. There are numerous ways of examining spontaneously ignitable materials but many of them can be very complicated and may be time consuming.

The mechanism of self-ignition of different materials involes the existence of exothermic reactions between these material and air/oxidizing agents which enters into their pores (in particle form), insterstices and occupy the void volume at normal ambient temperatures. A rise in the reactive system temperature occurs when any form of heat is released which increases the reaction of oxygen with additional molecules [11]. Storage size, oxygen diffusion conditions through the storage and product temperature at ambient are the three predominant parameters for self-ignition phenomenon [12]. Self-ignition of dust in bulk is caused by the rate of heat generation from oxidation and/or decomposition reactions of the dust being greater than the rate of heat loss. Generally, self-ignition or spontaneous combustion is limited to solid and gaseous materials with high specific surfaces. The thermal balance between the heat produced inside the dust mass and the heat loss from the environment are functions of the thermal conductivity and heat transfer coefficient on the outer surface of the dust with specified mass size [13]. This is attained either towards reaching a thermal equilibrium at a slightly higher temperature level or towards increasing the temperature of the dust mass until self-ignition. When the heat dissipation from the system is insufficient, heat production is superior to the overall heat loss. The different dust materials can accumulate around conveyor belts, machinery, plants, warehouses and so on; and can undergo self-heating and self-ignition [10].

There are five important properties of dusts that can affect the behaviour of a combustible dust. Properties that determine the characteristics of a combustible dust are its physical structure, chemical composition, electrical, thermal and optical properties [14]. The conditions that determine the spontaneous combustion of dust/powder materials include: (1) substance combustibility nature, (2) high surface area to enhance its reaction with oxygen when transported through the pores (3) presence of oxygen as the rate of heat production depends on oxygen partial pressure in the atmosphere, (4) substance or the surroundings temperature must be high enough for sufficient oxidation rate to influence heat production, (5) storage or deposit configuration must possess heat retaining capacity because dusts are very known to be of good heat insulators in practical situations, and lastly (6) residence time of the dust in a given storage or deposit configuration must be long enough to allow spontaneous combustion to take place [15]. Therefore, one of these six conditions should be eliminated or discarded to avoid spontaneous combustion. Fig. 1 presents a hexagon showing the self-ignition conditions of dusts. A self-ignition hexagon which is analogous to the fire triangle (consisting of fuel, oxygen and ignition) can be constructed as a conceptual tool representing the six main conditions that are needed to obtain self-ignition.

Several studies investigating the self-ignition attributes of dust/powder materials from cork powder carbonaceous stockpiles [16,17], crystalline silica [18], icing sugar, maize, bread-making flour, wheat, alfalfa, barley and soybean dusts [10], coal [8,19], calcium stearate [13] and sunflower and wood [9] have been conducted and their limitations and results were adequately presented. Several experimental methodologies used in achieving the aim and objectives of their studies include oxygen adsorption; crossing point measurements; temperature differential; isothermal and adiabatic calorimetry; differential scanning calorimetric and thermogravimetric [10,20].

In a similar study, Prodan et al. [9] investigated the self-ignition temperature of sunflower and wood powders dust accumulations. The dust from 1 m^3 of sunflower husks exhibited a self-ignition temperature that was higher than 62 °C such that 38 days will elapse before an ignition could occur if such volume is stored at this constant temperature. For the case of hardwood dust, 10 m^3 of the dust sample revealed a self-ignition temperature that was higher than 74 °C such that 68 h will elapse before an ignition could occur if such volume is stored at this constant temperature. It was concluded that heat production rate and the dust oxidation and/or decomposition reactions, higher than the heat loss rate, are the major causatives of self-ignition of bulk dust. The study conducted by Ramirez et al.

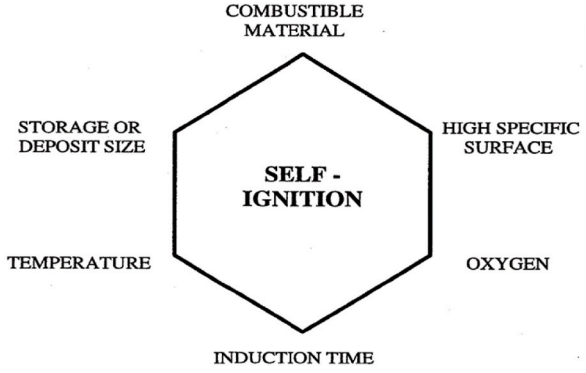

Fig. 1. Self-ignition hexagon of combustible dust materials [15].

[10] conducted the experimental determination of self-heating and self-ignition behaviour of dusts of agricultural materials such as bread-making flour, barley, wheat, maize, soybean, icing sugar and alfalfa kept in silos. It was concluded that these agricultural products can undergo oxidation and self-heating which may lead to fires and explosions.

Dowbysz et al. [21] determined the self-ignition characteristics of sludge dust and sludge pellets accumulation from the sewage sludge thermal drying station according to EN 15188. The result revealed the risk levels of the sludge dust and pellets in terms of their self-ignition attributes during their storage and transportation. It was revealed that the smallest basket volume of the sludge pellets and dust gave the highest self-ignition temperatures, which were 186 °C and 160 °C respectively. When the two forms of the thermally dried sludge were compared, authors suggested that the sludge dust exhibited the more favorable conditions in terms of fire risk despite the fact that the sludge pellets was easier to store and possess better handling issues.

The high consumption level of corn, wheat and rice due to their nutritional benefits to human has greatly influenced the volume of wastes generated from them which include the corn cob [22], wheat bran [23] and rice husk [24–27]. After the milling process in the food industry, the cob, bran and husk are kept in sacks and most times subjected to gasification. After a long period of time, they may catch fire resulting from their self-ignition potentials due to the presence of cellulose making them to be lignosellulosic in nature. Also, they contain multiple hydroxides which enhance their self-ignition ability as they can easily get oxidized in the presence of oxygen under ambient condition. Thus, there is need to investigate their self-ignition attributes under ambient condiction. In this study, isoperibolic hot storage experiments, as instructed in DIN EN 15188:2021 standard, at normal ambient conditions was adopted to obtain the temperature-time profiles of corn cob, wheat bran and rice husk dust samples at different oven temperatures using basket volume of 100 mL, 200 mL, 400 mL and 800 mL. Frank-Kamenetzkii's theory of thermal explosion was used to experimentally investigate the self-ignition temperature of corn cob, wheat bran and rice husk residues from biomass gasification. Dust samples were characterized via particle size distribution, proximate and ultimate analyses.

2. Materials and methods

2.1. Materials

2.1.1. Samples of dusty residues

Dusty residues of corn cob (Sample A), wheat bran (Sample B) and rice husk (Sample C) were obtained from dump sites of a food processing industry in Magdeburg, Germany after gasification and used without further grinding, drying and sieving. The DIN EN15188 standard method was adopted for the hot storage test to determine the self-ignition temperature (TSI).

2.1.2. Sample baskets

Fig. 2 shows various sizes of sample cubic baskets used in this study. The baskets are made of sintered metal, open at the top and closed at the bottom. The volume of each basket exceeded the volume of the preceding basket by a factor of 2. The volumes considered were 800 mL, 400 mL, 200 mL and 100 mL with respective half length (r) of 2.3 cm, 2.9 cm, 3.7 cm and 4.6 cm.

2.1.3. Laboratory oven

Fig. 3 shows the forced air-controlled convection laboratory oven (Memmert UFE500 115V) used for the isoperibolic (constant oven temperature) testing. The dimensions of the inside of the oven were 56 cm wide by 48 cm tall by 40 cm deep with an approximately 15 cm diameter fan on the back wall. The fan positioned at the back wall of the oven blew out across the back wall and not straightforward. There was a display and dial on the front that controlled the oven settings including the temperature, time, fan speed and maximum temperature of 300 °C. The inside of the oven was designed in a way that two thermocouples of type K are installed on opposite sides at 5 cm from the sample to measure the oven temperature. The third thermocouple is placed at the centre of the sample to measeure the samples' temperature. All the three thermocouples from the oven were connected to a central storage system which

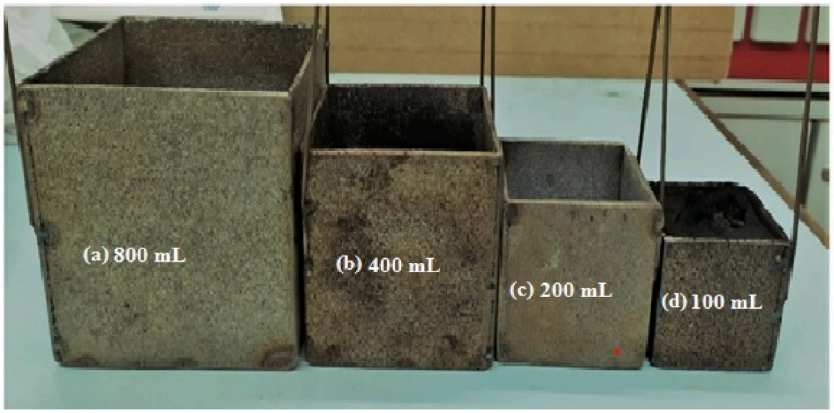

Fig. 2. Sample cubic baskets of (a) 800 mL (b) 400 mL (c) 200 mL and (d) 100 mL.

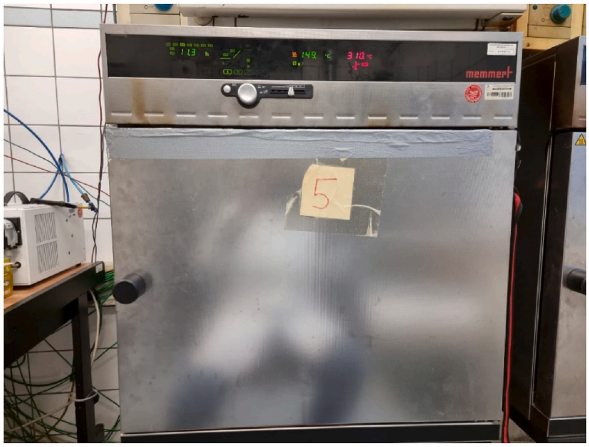

Fig. 3. Forced air-controlled convection laboratory oven.

was also connected to a computer through a cable. This system collected and stored the data for each test throughout the testing process. Measurements for all tests were taken automatically by the system at 30 s intervals.

2.2. Methods

2.2.1. Dust samples preparation and analysis

All the three dust samples were tested as obtained after gasification. Compositional analysis, residue determination and thermal stability of all samples was executed using a thermogravimetric analyser (TGA701LECO). The moisture contents was determined using a Sartorius moisture analyzer (MA45). The calorific values of all samples were also done using a calorimeter (IKA C200). A measurement of the rate of heat flow within a body/material for a specific change in temperature is called the thermal conductivity. FP2C conductivity meter (NeoTIM®, France) was utilized for the determination of the thermal conductivity of the dust samples under a temperature condition and a stable humidity environment. The particle size distribution of all the three dust samples was determined at 50 kPa dispersion pressure using a size distribution analyser (Retsch Camsizer XT) with the percentiles of the cumulative distribution at 32 % (D32), 50 % (D50) and 90 % (D90). For each test basket size, the bulk density ρ, was evaluated by weighing and recording the weights of empty basket (M_e) and filled basket (M_f) and divided by the basket volume (V_b) using Equation (1).

$$\rho = \frac{M_f - M_e}{V_b} \tag{1}$$

2.2.2. Hot storage test to determine self-ignition temperature

The experimental procedure used for this test was according to the European standard DIN EN 15188. The oven was turned on first so it could start its pre-heating process and reach the specified test temperature. After this, the dust sample with the settled bulk density is filled into the cubic basket with a spatula, without compressing and levelled on the top to remove any surplus dust from the upper margin. It was then checked again by weighing if the settled bulk density is reached with an accuracy of ±2 %. The cubic basket, being filled with the sample, is then positioned at the centre of the oven which has already been pre-heated to the test temperature. The experiment was repeated with the following equidistance sized volumes of 100, 200, 400 and 800 mL for all the three samples.

Two temperature measurements were recorded by three thermocouples and transmitted to the central storage devices during these tests. If sample temperature grows abruptly after an induction delay and rises at least 60K above the oven temperature, it is considered that self-ignition is occurring and the oven set temperature for that test is called the self-ignition temperature, TSI. On the other hand, we assume that self-ignition did not occur if sample temperature remains close to oven temperature after an induction delay or exceed it of a few K, i.e., less than 60K. Several numbers of tests were carried out with fresh dust sample for each trial, until the oven temperature is high enough to cause ignition of the sample, but which is no more than 2K higher than a temperature which fails to cause ignition. The self-ignition temperature (TSI) is defined as highest temperature at which a given volume of dust just does not ignite. The TSI is recorded for different oven temperatures, along with the time required for the oven temperature to be surpassed (the induction time, t_i). As the volume of the sample tested is increased, the TSI becomes lower, and the t_i becomes longer.

3. Results and discussion

3.1. Characterization of dust samples

Table 1 presents the proximate analysis, ultimate analysis, particle size distribution and bulk desity of dust samples examined in this study. Sample B possessed the highest moisture content of 2.08 % as compared to Samples A and C having 1.57 wt% and 1.41 wt%

respectively. The ash content and volatile content for Samples A, B and C are 37.99 wt%, 20.75 wt% and 15.82; and 19.88 wt%, 13.63 wt% and 7.21 wt% respectively. Sample C has the highest heating value (26895 kJ/kg), thermal conductivity (0.07 W/mK and bulk density (255.4 kg/m^3). The variations in the elemental compositions was due to the lignicellulosic nature of each of the dust samples.

3.2. Self-ignition temperature (TSI) - ignition time profile of dust samples

The self-ignition temperature (TSI) of dust samples was determine according to DIN EN15188:2021 where it was stated that the TSI lies between the highest oven temperature without ignition and the oven temperature at which the dust just ignited. Also, evaluated was the ignition time (t_i) which was defined as the time interval between reaching the oven and ignition temperature. This was evaluated as the time of maximum temperature jump within the sample due to the abrupt rise in temperature during ignition.

The temperature-time profiles of dust samples at different oven temperatures using basket volume of 100 mL, 200 mL, 400 mL and 800 mL are presented as Figs. 4–7 respectively. It was observed that the curves for the different sample sizes became wider as the basket volume was increased from 100 mL to 800 mL. This was due to the higher proportion of dust that was available for incineration. In addition, the influence of the volume sizes on the ignition temperature and ignition time can be deduced from the plot. As shown in Fig. 4, the ignition temperature for Samples A, B and C was 235 °C, 210 °C and 240 °C at ignition time of 48 min, 46 min and 44 min respectively. From the samples examined, Sample C exhibited the highest ignition temperature at lowest ignition time. The result revealed twice the ignition time for each samples when the basket volume was increased to 200 mL (Fig. 5). However, the oven temperature at ignition dropped to 223 °C, 198 °C and 220 °C for samples A, B and C respectively at ignition time of 53 min, 50 min and 48 min. Similar trend was observed for dust samples in 400 mL (Fig. 6) and 800 mL (Fig. 7) with longer ignition time. For basket volume of 400 mL, the ignition temperature was 212 °C, 188 °C and 192 °C for Samples A, B and C respectively at ignition time of 64 min, 61 min and 59 min. For basket volume of 800 mL, the ignition temperature was 202 °C, 180 °C and 174 °C for Samples A, B and C respectively at ignition time of 116 min, 79 min and 71 min. This indicated the influence of the volume size of the dust deposit on the ignition time and temperature of the samples examined. This can be explained by the fact that less heat can be accumulated in thin layers of dust than in thick layers. As the sample temperature increases, the reaction rate also increases. This resulted in a runaway reaction occurring as one could notice the abrupt rise in the dust temperature after the heating process. At this point there was a competing oxidation and pyrolysis reactions going on within the deposit resulting in a self-sustained smouldering fire which begins to spread and consume the dust. If the oxygen supply at the middle of the basket is inadequate, the pyrolysis process is the dominating reaction at this point. Generally, the ignition temperature decreases with increase in ignition time as the dust basket volume was increased. Hence, it is important for determining the self-ignition temperature of the dust deposit. Table 2 summarizes the ignition temperature, ignition time and maximum temperature reached by dust samples at different volume.

Generally, all the water contents in the samples were relatively low. Also, moisture content does not affect the value of self-ignition temperature, but only impacts the time taken to achieve self-ignition [28]. The lowest self-ignition temperature for the dust samples was 180 °C. The highest self-ignition temperature was observed in sample C with a temperature of 240 °C. The dependence of the auto-ignition temperature on the volume of sample C was the greatest of all the samples and thus, it could be considered as the most hazardous. This could be observed in the flat rise of the curve in the Arrhenius plot and evident in the associated very low activation energy.

In Fig. 7, Sample C exhibited a different temeperature-time profile behavior at dust basket volume of 800 mL. The sample was heated at an oven temperature of $T_{ov} = 172$ °C (445K). The sample temperature and the temperatures of the two thermocouples were then plotted against time. The sample initially had a temperature of about 25 °C and after less than 10 min of heating, it experienced an

Table 1
Characterization of dust samples.

Properties	Residue Dust Samples		
	Sample A	Sample B	Sample C
Proximate analysis (wt.%)			
Moisture Content	1.57	2.08	1.41
Ash	37.99	20.75	15.82
Volatile Content	19.88	13.63	7.21
Ultimate analysis			
Thermal conductivity (W/m/K)	0.05	0.06	0.07
Carbon (wt.%)	54	72.01	78.97
Hydrogen (wt.%)	0.16	0.68	0.57
Nitrogen (wt.%)	1.16	1.28	1.16
Oxygen (wt.%)	5.12	3.2	2.07
Sulphur (wt.%)	0	0	0
Heating Value (KJ/Kg)	15889	23653	26895
Bulk Density (Kg/m^3)	171.2	217.2	255.4
Particle size distribution			
D32 (mm)	2.369	0.0178	0.1938
D50 (mm)	2.738	0.0304	0.3387
D90 (mm)	4.314	0.2594	0.7568

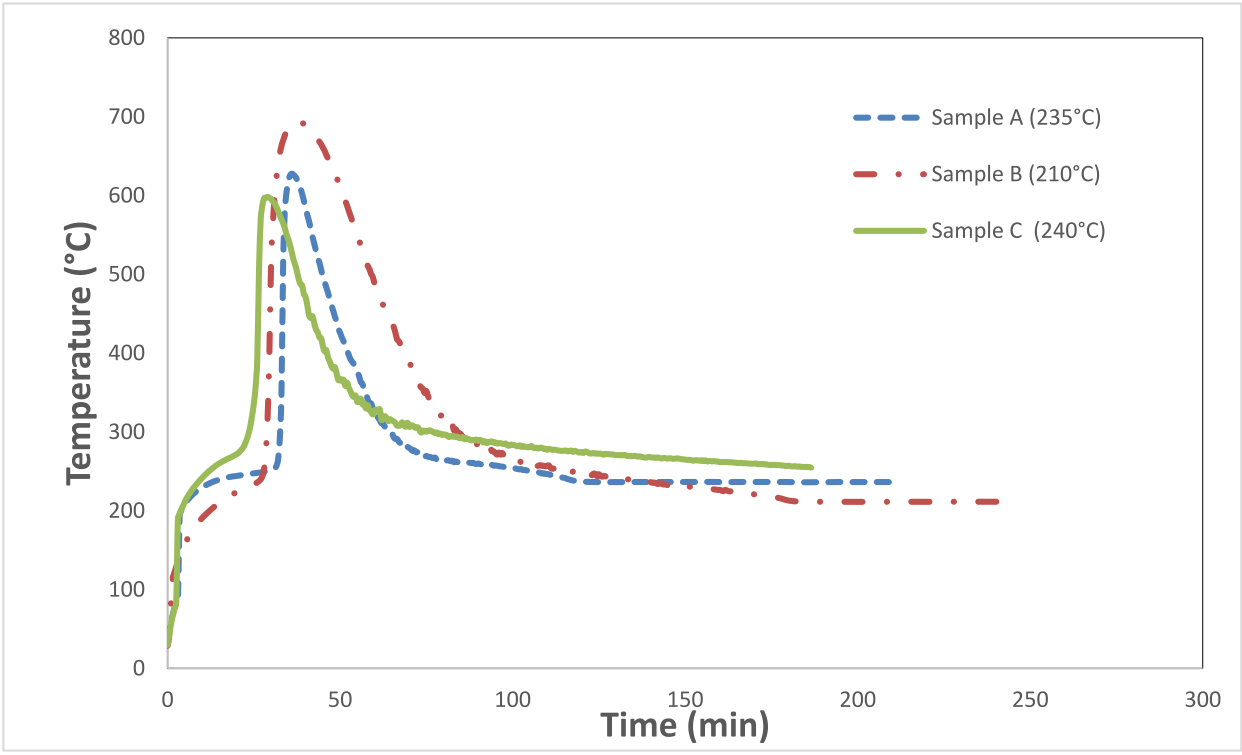

Fig. 4. Temperature-time plot of dust samples at different oven temperatures with basket volume of 100 mL.

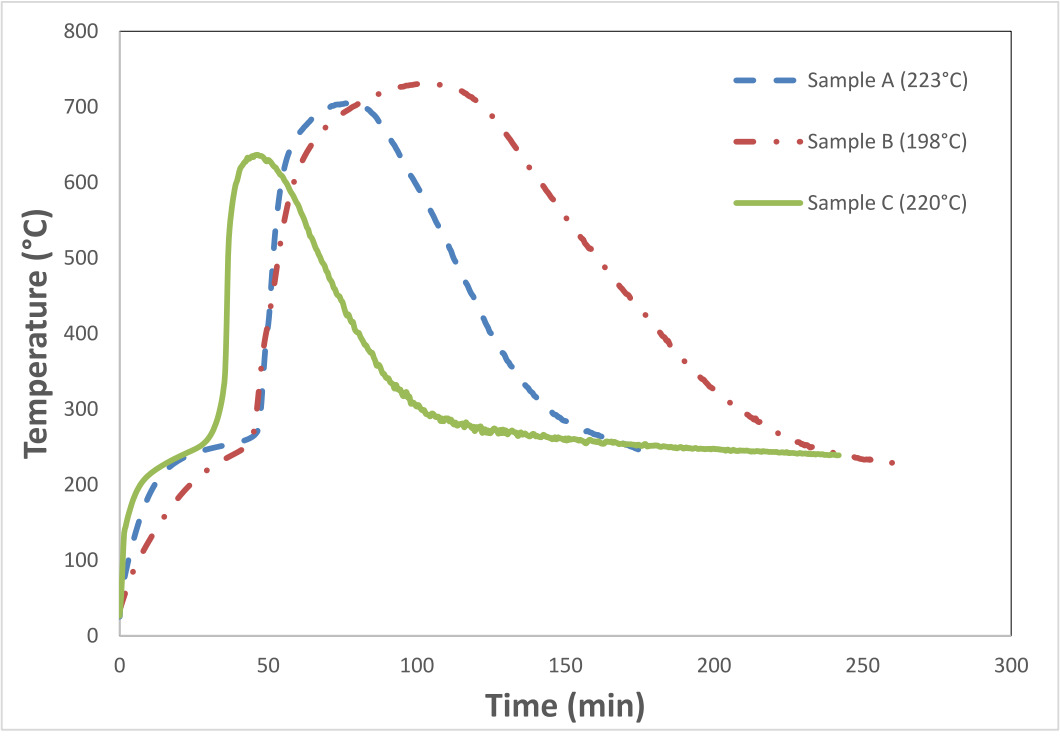

Fig. 5. Temperature-time plot of dust samples at different oven temperatures with basket volume of 200 mL.

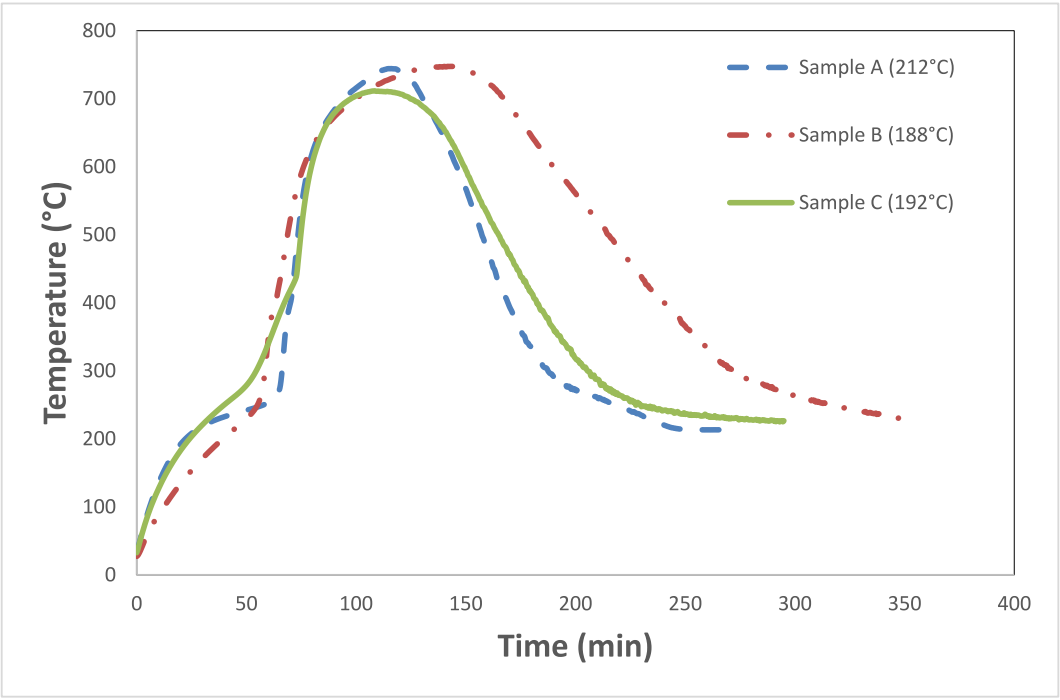

Fig. 6. Temperature-Time plot of dust samples at different oven temperatures using a basket volume of 400 mL.

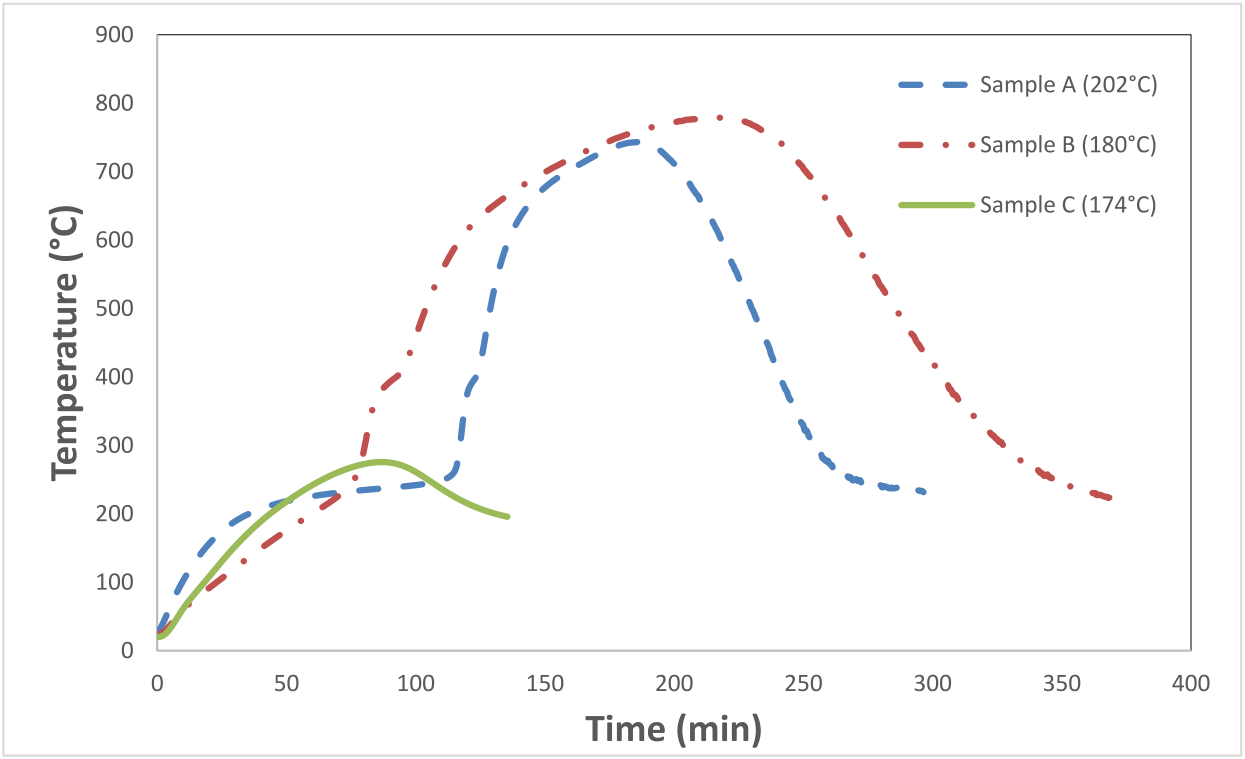

Fig. 7. Temperature-Time plot of dust samples at different oven temperatures using a basket volume of 800 mL.

Table 2
The ignition temperature and ignition time of dust samples at different volume.

Sample	Property	Volume (mL)			
		100	200	400	800
A	Ignition Temperature (°C)	235	223	212	202
	Ignition Time (min)	48	53	64	116
	Maximum Temperature (°C)	620.58	691.19	728.99	751.20
B	Ignition Temperature (°C)	210	198	188	180
	Ignition Time (min)	46	50	61	79
	Maximum Temperature (°C)	669.89	728.16	745.02	778.68
C	Ignition Temperature (°C)	240	220	192	174
	Ignition Time (min)	44	48	59	71
	Maximum Temperature (°C)	587.96	623.67	708.32	273.36

inflection point just above 30 °C. This inflection point occurred below the oven temperature, and the heating process proceeded. After heating for approximately 40 min the sample temperature T_s was equal to the oven temperature. Subsequently, a notable increase in the sample temperature was observed above the oven temperature (about 35K above the oven temperature), that is self-heating. This increase was caused by an increase in the exothermic reaction rate, which allowed for a further temperature rise as positive feedback. However, since the heat transfer resistance within the dust deposit could not restrict the heat transfer to the surroundings, the heat produced at the oven temperature was not enough to initiate a runaway reaction. Hence, after about 120 min (1 h) a steady state was achieved at temperatures slightly above the oven temperature. No ignition was observed as the process did not meet the ignition criteria. After taking out the sample from the oven, it remained unchanged with very little mass loss when weighed. At 174 °C, a change in the nature of temperature curve of sample C was noticed with sudden reduction in the ignition time with lowered temperature when compared with the temperature curves of samples A and B. At this point, the 60 K temperature rise could have been exceeded. Asides this point where the maximum temperature reached by sample C was drastically reduced to 273.36 °C, increase in the maximum temperature reached by each of the samples A, B and Cwas noticed as basket volume was increased from 100 mL to 800 mL. The maximum temperature reached, increased from 620.58 °C, 669.89 °C and 587.96 °C–751.20 °C, 778.68 °C and 708.32 °C for samples A, B and C respectively as presented in Table 2.

3.3. Arrhenius plot of dust samples using Frank Kamenetzkii (FK) method

The results of the experiments were evaluated using advanced Frank Kamenetzkii (FK) method which is based on the theory of thermal explosion. The assumptions which constitute the basis of the stationary Frank-Kamenetskii theory include: (1) heat generation is via a single reaction whose rate at a given temperature is not a function of time, (2) the activation energy is assumed to be sufficiently high, (3) heat transfer through the body is by conduction only, (4) heat transfer at the boundaries to the surrounding is taking place through convection and radiation, and (5) the material is assumed to be isotropic and homogeneous with constant physical properties. The Frank-Kamenetskii parameter δ also known as the dimensionless reaction velocity as it includes all characteristics of the dust deposit, and the reactive system is given as Equation (2):

$$\delta = \frac{E \cdot r^2 \cdot \rho \cdot Q \cdot k_0}{\lambda \cdot R \cdot T_a^2} \cdot \exp\left(-\frac{E}{R \cdot T_a}\right) \tag{2}$$

where E is the apparent activation energy of the combustion reaction, r is the characteristic length of the deposit (e.g., radius of a cylinder or sphere or half the thickness of a slab), ρ is the bulk density, Q is the heat of reaction per unit mass, λ is the thermal conductivity of the bulk material, R is the universal gas constant, T_a is the ambient temperature of the deposit, and k_0 is the pre-exponential factor of the Boltzmann term exp (-E/R T_a).

The linearized form of Equation (2) is stated as Equation (3) (which can be correlated with Equation (4)) which was used in making a linear plot presented in Fig. 8. Depending on the geometry of the dust deposit, the ambient temperature is equal to its TSI when a maximum value of the FK parameter is inserted in Equation (2). This means that when $\ln\left(\delta\frac{T^2}{r^2}\right)$ vs $\frac{1}{T_a}$ is plotted in a diagram such that

Where $\delta = 2.52$, the measured values of TSI in the sample dust deposit of various sizes follows a straight line. The slope provides an estimate of the apparent activation energy of the combustion process and this line can be extrapolated to larger deposit volumes. The FK model as well allows for the establishment of a relationship between self-ignition temperature and storage size. Then, extrapolation from this connection can assist in evaluating: 1) the critical size (maximum size) of a storage at a specific temperature, which is especially beneficial for low temperatures, for varied storage geometries; and 2) the maximum storage temperature (critical storage temperature) for the chosen size and geometry.

$$\ln\left(\delta_c\frac{T_a^2}{r^2}\right) = -\frac{E}{R}\cdot\frac{1}{T} + \ln\left(\frac{E \cdot Q \cdot \rho \cdot k_o}{R \cdot \lambda}\right) \tag{3}$$

$$y = mx + n \tag{4}$$

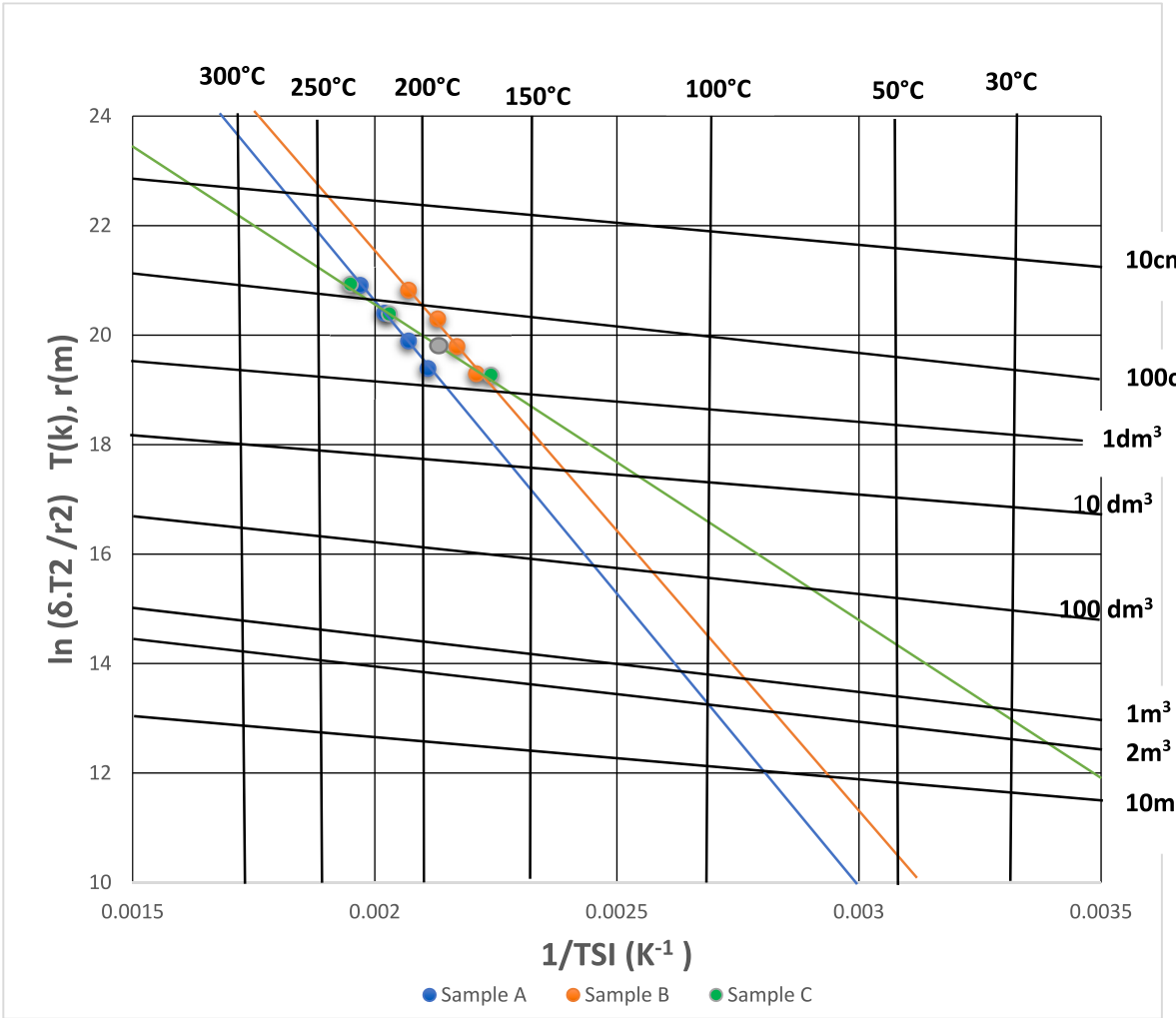

Fig. 8. Arrhenius plot for the self-ignition behaviour of all dust samples using the model of Frank-Kamenetzkii.

Fig. 8 represents the Arrhenius plot for the self-ignition behaviour of all dust samples using the model of Frank-Kamenetzkii. The graphical representation follows a straight line. Consequently, using Equation (3), the apparent activation energy E/R can be derived from the slope and the exponential term, n, can be determined from the intercept of the FK Arrhenius diagram. The pre-exponential factor, k_o, can also then be calculated as well from n when all other properties of the sample are known. The result presented in Fig. 8 revealed the self-ignition temperature of sample A in a bigbag of 1 m^3 storage volume to be approximately 105 °C and 100 °C for a bigbag of 2 m^3 storage volume respectively. The self-ignition temperature of sample B in a bigbag of 1 m^3 storage volume is approximately 90 °C and 85 °C for a bigbag of 2 m^3 storage volume. Similarly, the self-ignition temperature of sample C in a bigbag of 1 m^3 storage volume is approximately 35 °C and for the 2 m^3 bigbag it is 25 °C. The pre-exponential factor, k_o was calculated as 3.32×10^6 S^{-1}, 8.33×10^6 S^{-1} and 1.2×10^2 S^{-1} for sample A, B and C respectively. Table 3 shows the activation energies and exponential term of all dust samples. The activation energy is the minimum energy required to initiate a reaction or reach a transition state. The activation energy, E, required for the ignition of the sample dust was highest in sample B (90.90 kJ/mol) and lowest in sample C (46.52 kJ/mol). This also implies that the higher the activation energy, then the higher is the TSI required for the onset of the spontaneous ignition for a given size of the dust. The values of the correlation coefficient for the Arrhenius plot for the self-ignition behaviour of all

Table 3
Activation energies and exponential terms of all dust samples.

	Linear Equation	R^2	E/R (K)	E (KJ/mol)	n (K^2/m^2)
Sample A	y = −10753x+ 42.11	0.9976	10753	89.40	42.11
Sample B	y = −10933x + 43.5	0.9910	10933	90.90	43.5
Sample C	y = −5595.7x+ 31.81	0.9962	5595.7	46.52	31.81

dust samples using the model of Frank-Kamenetzkii are also presented in Table 3. R^2 values of 0.9976, 0.9910 and 0.9962 were recorded for Samples A, B and C respectively.

4. Conclusions

The self-ignition attributes of corn cob, wheat bran and rice husk residues in ambient air from biomass gasification was investigated via the evaluation of their self-ignition temperatures and kinetic parameters using DIN EN 15188:2021 standard and Frank-Kamenetzkii's theory of thermal explosion respectively at varying basket volume. The results revealed decrease in the ignition temperature of dust samples as ignition time and dust basket volume were increased. Sample C was considered to be the most hazardous with respect to its propensity to self-heating possessing the lowest self-ignition temperature of 173 °C at 800 mL cubic mesh. The moisture contents in sample C was 1.41 %, the lowest among all the three samples. Also, Sample C (rice husk) exhibited the highest thermal conductivity, carbon content, heating value and bulk density. The activation energy, *E*, required for the ignition of the sample dust was highest in sample B (90.90 kJ/mol) and lowest in sample C (46.52 kJ/mol). The higher the activation energy, the higher the TSI required for the onset of the spontaneous ignition for a given size of the dust. The values of the correlation coefficient (R^2 values) for the Arrhenius plot for the self-ignition behaviour of all dust samples using the model of Frank-Kamenetzkii were 0.9976, 0.9910 and 0.9962 for Samples A, B and C respectively. In conclusion, the data presented in this study is not universally applicable to all dust residues but effective and valid alone in predicting the self-ignition ability of corn cob, wheat bran and rice husk residues in ambient air from biomass gasification in order to prevent sudden fire attack that may arise based on storage of their dust particles in food processing industries.

Ethical approval

This declaration is not applicable.

Funding

No financial support in form of funding was received for the execution of this research work.

Data availability statement

Data will be made available on request.

CRediT authorship contribution statement

Moses Oshiomah Osibuamhe: Supervision, Resources, Project administration, Methodology, Investigation, Formal analysis, Data curation, Conceptualization. **Lekan Taofeek Popoola:** Writing – review & editing, Writing – original draft, Visualization, Validation. **Yuli Panca Asmara:** Resources. **Usman Taura:** Supervision, Funding acquisition. **Tajudeen Adejare Aderibigbe:** Data curation.

Declaration of competing interest

The authors declare that they have no known competing financial interests or personal relationships that could have appeared to influence the work reported in this paper.

Acknowledgement

The first author appreciates the support from Otto-Von-Guericke University, Magdeburg, Germany for creating enabling environemnet to conduct the research work. The second author appreciates the support rendered by INTI International University, Malaysia towards the publication of this article.

References

[1] S. Yin, Y. Du, X. Liang, Y. Xie, D. Xie, Y. Mei, Surface coating of biomass-modified black phosphorus enhances flame retardancy of rigid polyurethane foam and its synergistic mechanism, Appl. Surf. Sci. 637 (2023) 157961, https://doi.org/10.1016/j.apsusc.2023.157961.

[2] C. Zhu, M. Wang, M. Guo, J. Deng, Q. Du, W. Wei, Y. Zhang, A. Mohebbi, An innovative process design and multi-criteria study/optimization of a biomass digestion- supercritical carbon dioxide scenario toward boosting a geothermal-driven cogeneration system for power and heat, Energy 292 (2024) 130408, https://doi.org/10.1016/j.energy.2024.130408.

[3] H. Li, T. Zhang, S.M. Shaheen, H. Abdelrahman, E.F. Ali, N.S. Bolan, G. Li, J. Rinklebe, Microbial inoculants and struvite improved organic matter humification and stabilized phosphorus during swine manure composting: multivariate and multiscale investigations, Bioresour. Technol. 351 (2022) 126976, https://doi.org/10.1016/j.biortech.2022.126976.

[4] T. Zhang, H. Li, T. Yan, S.M. Shaheen, Y. Niu, S. Xie, Y. Zhang, H. Abdelrahman, E.F. Ali, N.S. Bolan, J. Rinklebe, Organic matter stabilization and phosphorus activation during vegetable waste composting: multivariate and multiscale investigation, Sci. Total Environ. 891 (2023) 164608, https://doi.org/10.1016/j.scitotenv.2023.164608.

[5] Renewable Energy Directive, Directive 2009/28/EC of the European Parliament and of the Council of 23 April 2009 on the Promotion of the Use of Energy from Renewable Sources and Amending and Subsequently Repealing Directives 2001/77/EC and 2003/30/EC, 2009, pp. 16–62.

[6] Y. Feng, J. Chen, J. Luo, Life cycle cost analysis of power generation from underground coal gasification with carbon capture and storage (CCS) to measure the economic feasibility, Resour. Pol. 92 (2024) 104996, https://doi.org/10.1016/j.resourpol.2024.104996.
[7] Y. Du, X. Liu, L. Chen, S. Yin, Y. Xie, A. Li, X. Liang, Y. Luo, F. Wu, Y. Mei, D. Xie, 3D hierarchical fire proof gel polymer electrolyte towards high-performance and comprehensive safety lithium-ion batteries, Chem. Eng. J. 476 (2023) 146605, https://doi.org/10.1016/j.cej.2023.146605.
[8] D. Wu, M. Schmidt, J. Berghmans, Spontaneous ignition behaviour of coal dust accumulations: a comparison of extrapolation methods from lab-scale to industrial-scale, Proc. Combust. Inst. 37 (3) (2019) 4181–4191.
[9] M. Prodan, A. Szollosi-Moța, V.I. Nälboc, N.S. Șuvar, A. Jurca, Self-ignition temperature of the dust accumulations for sunflower and wood powder, MATEC Web Conf. 354 (1) (2022) 12–21.
[10] A. Ramírez, J. García-Torrent, A. Tascón, Experimental determination of self- heating and self-ignition risks associated with the dusts of agricultural materials commonly stored in silos, J. Hazard Mater. 175 (1–3) (2010) 920–927.
[11] T. Abbasi, S. Abbasi, Dust explosions – cases, causes, consequences, and control, J. Hazard Mater. 140 (2007).
[12] A. Janes, D. Carson, A. Accorsi, J. Chaineaux, B. Tribouilloy, D. Morainvillers, Correlation between self-ignition of a dust layer on a hot surface and in baskets in an oven, J. Hazard Mater. 159 (2–3) (2008) 528–535.
[13] N.S. Suvar, M. Prodan, I. Nalboc, R. Szollosi-Mota, M.C. Suvar, Determination of spontaneous ignition behaviour of Calcium Stearate dust accumulation, IOP Conf. Ser. Earth Environ. Sci. 609 (1) (2020) 12056–12064.
[14] R. Eckhoff, Dust Explosions in the Process Industries, third ed., Gulf Professional Publishing, Burlington, 2003.
[15] D. Carson, A methodological approach to the spontaneous combustion of agricultural dusts, in: International Symposium on Hazards Prevention and Mitigation of Industrial Explosions, Jun 1996, 1996, pp. 311–324. Bergen, Norway.
[16] M.A. Smith, D. Glasser, Spontaneous combustion of carbonaceous stockpiles Part I: the relative importance of various intrinsic coal properties and properties of the reaction system, Fuel 84 (2005) 1151–1160.
[17] H. Zoghlami-Mosrat, A. Laurent, J.P. Corriou, A priori characterization of criticity and of dynamic thermal behaviour of a storage of cork powder, Chem. Eng. Res. Des. 86 (2008) 640–647.
[18] A. Maciejewska, Occupational exposure assessment for crystalline silica dust: approach in Poland and worldwide, Int. J. Occup. Med. Environ. Health 21 (1) (2008) 1–23.
[19] F. Su, X. He, M. Dai, J. Yang, A. Hamanaka, Y. Yu, L. Wen, J. Li, Estimation of the cavity volume in the gasification zone for underground coal gasification under different oxygen flow conditions, Energy 285 (2023) 129309, https://doi.org/10.1016/j.energy.2023.129309.
[20] J.N. Carras, B.C. Young, Self-heating of coal and related materials: models, application and test methods, Prog. Energy Combust. Sci. 20 (1) (1994) 1–15.
[21] A. Dowbysz, B. Kukfisz, M. Samsonowicz, J.S. Bihałowicz, Determination of the self- ignition behavior of the accumulation of sludge dust and sludge pellets from the sewage sludge thermal drying station, Energies 16 (2023) 46.
[22] B. Huma, M. Hussain, C. Ning, Y. Yuesuo, Human benefits from maize, Sch J Appl Sci Res 2 (2) (2019) 1–4.
[23] R.B. Chalamacharla, K. Harsha, K.B. Sheik, C.K. Viswanatha, Wheat bran- composition and nutritional quality: a review, Adv. Biotech & Micro. 9 (1) (2018) 555754.
[24] L.T. Popoola, Nano-magnetic walnut shell-rice husk for Cd(II) sorption: design and optimization using artificial intelligence and design expert, Heliyon 5 (2019) e02381.
[25] L.T. Popoola, Characterization and adsorptive behaviour of snail shell-rice husk (SS-RH) calcined particles (CPs) towards cationic dye, Heliyon 5 (2019) e01153.
[26] L.T. Popoola, Tetracycline and sulfamethoxazole adsorption onto nanomagnetic walnut shell-rice husk: isotherm, kinetic, mechanistic and thermodynamic studies, Int. J. Environ. Anal. Chem. 100 (9) (2020) 1021–1043.
[27] L.T. Popoola, T.A. Aderibigbe, A.S. Yusuff, M.M. Munir, Brilliant green dye adsorption onto composite snail shell–rice husk: adsorption isotherm, kinetic, mechanistic and thermodynamic analysis, Environ. Qual. Manag.28 (2) (2018) 63–78.
[28] H. Park, A.S. Rangwala, N.A. Dembsey, A means to estimate thermal and kinetic parameters of coal dust layer from hot surface ignition tests, J. Hazard Mater. 168 (2009) 145–155.